

Size distribution modeling for fluidized bed solar-grade silicon production

Christy M. White, Paul Ege*, B. Erik Ydstie

Department of Chemical Engineering, Carnegie Mellon University, Pittsburgh, PA 15217

Abstract

This work addresses modeling size distribution of solar-grade silicon particles grown by thermal decomposition of silane gas in a fluidized bed reactor. Particles grow with heterogeneous chemical vapor deposition and by scavenging powder produced in homogeneous gas phase reaction. The model uses ordinary differential and algebraic equations that track particle movement through discrete size intervals to simulate changes in the size distribution. The model solves quickly and is easily tuned to fit experimental data. Validating the model with experimental data from pilot plant tests shows that this approach is useful for control system design and scale-up of the fluidized bed silicon production process. Combining the developed model with feedback control theory also provides a novel method for sensitivity analysis.

Keywords: population balance, silane, fluidization, solar-grade silicon

*Solar Grade Silicon LLC, Moses Lake, WA 98837

This paper was presented at the AIChE Annual Convention in Austin, TX, 2004.

1 Introduction

The silicon industry has considered thermal decomposition of silane (SiH_4) gas to solid silicon and hydrogen gas in a fluidized bed reactor a potentially viable method of high-purity silicon production for several years. Until recently, the fluidized bed process was not developed for production. The micro-electronics industry has been able to afford trichlorosilane (SiHCl_3) decomposition in a Siemens-type reactor, which costs \$40-\$65/kg as a result of batch processing and high energy requirements. This cost is too high for the photovoltaics (PV) industry (Woditsch & Koch 2002), which has been growing as much as 30% annually in recent years. Off-spec or by-product silicon generated during micro-electronics manufacturing is used as feedstock for the PV industry, but that supply is diminishing since the electronics industry has not experienced the growth of the PV industry. The cost of producing solar-grade feedstock constitutes about 20% of the total cost of solar cell production. So, developing an affordable source of solar-grade silicon will contribute to the growth of the PV industry. To achieve such a goal, silicon production in a fluidized bed reactor is receiving renewed attention from companies such as Solar Grade Silicon in Washington State.

The feasibility of high-purity silicon production in a fluidized bed reactor to reduce capital and operating costs has been studied in several laboratory-scale investigations. Hsu et al. (1987) were able to identify factors that affect the size of silicon particles produced as well as equipment that controls those factors. They also evaluated reactor performance for a variety of conditions. Caussat et al. (1995*a*) completed additional experiments of fluidized bed silicon production. They operated under slightly different conditions (e.g. smaller particles) and observed new phenomena such as changes in fluidization quality caused by silane addition. More recently, Tejero-Ezpeleta et al. (2004) completed experiments to determine optimal operating conditions for commercial production of solar-grade silicon. In one of several studies of low-pressure polysilicon film deposition, Zambov (1992) identified the rate of homogeneous silane decomposition. Additionally, Lai et al. (1986), Furusawa et al. (1988) and Caussat et al. (1995*b*), among others, worked to develop rate expressions for silane decomposition in fluidized bed reactors through both heterogeneous and homogeneous pathways. These and other efforts provide a solid theoretical foundation for the development of a commercial fluidized bed process.

Fluidized bed reactor dynamics are characterized by the production, growth, or decay of discrete particles contained in a continuous phase. Examples of processes in which this type of behavior is important include crystallization, production and growth of atmospheric aerosols or biological cells, granulation, and fluidized bed vapor decomposition. Our aim is to establish a dynamical model of the fluidization process which can be used to develop control strategies and study dynamic stability. A particulate process has properties that are distributed along both external and internal coordinates. The external coordinates are space and time. The internal coordinates are particle properties such as size or age. In the framework of this phase space, Hulburt and Katz (1964) used the theory of statistical mechanics to develop a continuous phase space description of the particulate system behavior. The so called population balance equation describes particles' evolution in phase space. The population balance equation expresses the "conservation of probability" (e.g. number density of particles) in the phase space.

The set of equations that results from the combination of the population balance equation with mass balance equations for the continuous phase is often difficult to solve, because it can include partial integrodifferential equations (Dueñas Diez et al. 2002). Moment transformation and discretization are two commonly used methods of solution. Randolph & Larson (1988) proposed the use of moment transformation to solve such systems. Adams & Seinfeld (2002) used a two-moment approach to predict aerosol size distributions. Weimer & Clough (1980) used or-

thogonal collocation to solve a system of equations representing char gasification in a fluidized bed reactor. Also, Hounslow (1990), Henson et al. (2002) and Immanuel & Doyle III (2003) employed different discretization techniques to predict crystal, cell, and polymer growth, respectively. Most solution methods employed first simplify the continuous population balance equation. A tractable approximation of the equation is then obtained and solved for given conditions. One problem with such discretization schemes is that the conservation principles may not hold exact for very precise gridding (Adams & Seinfeld 2002). Another related problem is that the methods may be computationally expensive.

This work addresses modeling and analysis of particulate processes using a discrete representation of the phase space. The approach simplifies the modeling task, ensures that conservation laws are maintained at all discretization levels, and facilitates computation without additional discretization. In the limit of infinitely fine discretization, we obtain the classical population balance model. The method can therefore be viewed as a physically based discretization scheme with an additional constraint, which accounts for the number balance. Using silicon production in a fluidized bed reactor as a case study, we have developed a model for some properties of particulate processes. The newly developed fluidization process is described in Section 2. The derivation of the model is presented in Section 3. The relationship between the discrete model and the population balance equation is established in Section 4. The model was validated against pilot plant data from Solar Grade Silicon by tuning adjustable parameters to predict behavior more accurately. The data collection and accuracy of model predictions, which indicate that this modeling approach is practical, are presented in Section 5. Using the validated model and feedback control theory to simulate continuous operation of the reactor provides a novel way to investigate reactor performance at a variety of conditions, and the results are discussed in Section 6.

2 Process Description

A schematic presentation of silane decomposition in a fluidized bed reactor is shown in Figure 1. Silane and hydrogen gases enter at the bottom of the reactor with sufficient space time velocity to fluidize the bed of silicon particles. Wall heaters and preheated gas streams heat the fluidized bed to maintain required reaction temperatures. When silane gas is heated, it thermally decomposes to solid silicon and hydrogen gas. Most of the solid silicon deposits on the surface of the particles in the reactor, causing the particles to grow. The hydrogen gas and some entrained silicon powder

exit the top of the reactor. During continuous production, silicon product will be removed from the reactor to ensure mass balance while seed particles will be added or generated to ensure constant average particle size.

The fluidized bed reactor is governed by the overall reaction, $\text{SiH}_{4(g)} \rightarrow \text{Si}_{(s)} + 2\text{H}_{2(g)}$. Silane (SiH_4) gas thermally decomposes to solid silicon and hydrogen gas through two different mechanisms. Silane undergoes heterogeneous chemical vapor deposition when it reacts at the surface of solid silicon and forms a gray, crystalline solid. Silane undergoes homogeneous reaction when it reacts with other silane molecules in the gas phase to form a brown, amorphous powder. Some powder is scavenged by existing particles and then re-crystallized to contribute to particle growth. The remainder is exhausted with hydrogen and thereby reduces the overall yield. One important objective of this study is to develop models and control mechanisms that can be used to improve yield by minimizing powder loss in a commercial production system.

3 Model Development

The concept of Hulburt and Katz's (1964) particle phase space is illustrated in Figure 2. The entire process is distributed across space and time, but the particles are also distributed across an internal coordinate axis of size, age, or other quantity. They developed a model framework based on statistical mechanics and an infinite dimensional representation of the particle dynamics. Our approach is developed from a discrete representation of the particulate system. Macroscopic mass and number balances are performed over discrete size intervals to simulate changes in the particle size distribution. The size distribution equation models the internal size coordinate, and mass balance equations model external space and time coordinates. The combination of the equations produces a finite dimensional computer model that can be used to simulate processes such as silane decomposition in a fluidized bed reactor. We show that our model converges to the classical population balance model if we allow the number of discretization intervals to increase to infinity.

The model we develop assumes that all reaction takes place in the dense fluid bed section of the reactor, shown in Figure 1. Reaction in the reactor freeboard is neglected. Equations for the rate of silane decomposition have been obtained from the work of Lai et al. (1986). They combine an expression from Iya et al. (1982) for heterogeneous decomposition and an expression

for homogeneous reaction from Hogness et al. (1936) to give

$$\begin{aligned} R_{het} &= 2.79 \times 10^8 e^{(-19530/T)} C_s V_g \\ R_{hom} &= 2 \times 10^{13} e^{(-26000/T)} C_s V_g. \end{aligned} \quad (1)$$

Silicon production is expressed in units of moles per second in the above equations. The reaction depends on the silane concentration, C_s , and the volume of gas, which is the difference between the volume of the reaction zone and the volume of solids ($V_g = V - V_s$). The volume of solids is calculated with the density of silicon, and we assume that the particles' porosity is negligible, so $V_s = M/\rho$, when M is the total mass of silicon. As shown in Figure 1, it may be necessary to account for loss of product as powder can be entrained and removed from the reactor. Silicon particles in the reactor grow with heterogeneous decomposition and by scavenging a fraction of the silicon powder produced through homogeneous decomposition. The remaining powder is exhausted. So, the powder mole balance is

$$\frac{dM_p}{dt} = R_{hom} - R_{loss} - R_{sc}.$$

We assume the rate of powder scavenging is proportional to the concentration of silicon powder produced so that

$$R_{sc} = k_{sc} C_p. \quad (2)$$

Here, C_p is defined as the moles of powder divided by the volume of gas in the reactor. Some or all of the powder may be scavenged by particles, so the range of values of the adjustable proportionality constant is $0 \leq k_{sc} \leq V_g \text{ m}^3/\text{s}$. The correct value can be determined by comparing model predictions with experimental data.

A steady-state analysis of the powder mole balance allows definition of the rate of loss of silicon powder (R_{loss}) out the top of the reactor, which is

$$R_{loss} = R_{hom} - k_{sc} C_p. \quad (3)$$

The total rate of solids production is the combination of the heterogeneous product and the scavenged powder, meaning

$$R = R_{het} + R_{sc}. \quad (4)$$

The model we develop is based on the assumption that the reactants, the silane gas and silicon particles, are completely mixed. While this is a coarse assumption, it has been verified experimentally that silicon particles are vigorously stirred by the gaseous components. Equations (5) and (6) below represent the changes in silane and hydrogen concentrations respectively.

$$\frac{d(V_g \cdot C_s^{out})}{dt} = F^{in} \cdot C_s^{in} - F^{out} \cdot C_s^{out} - (R + R_{loss}) \quad (5)$$

$$\frac{d(V_g \cdot C_h^{out})}{dt} = -F^{out} \cdot C_h^{out} + 2 \cdot (R + R_{loss}) \quad (6)$$

Here, F^{in} and F^{out} represent the total gas flow into and out of the reactor.

Figure 3 illustrates the modeling technique applied to the solid silicon particles. A key assumption for this analysis is that particles are distributed among size intervals characterized by an average number of moles, m_i . A few different events cause particles to move between size intervals. In the silicon fluidized bed reactor, the most obvious driving force for a change in the size distribution is that reaction occurs and causes the particles to grow from one characteristic size to the next. The distribution of the product of reaction into each size interval is represented by r_i . The resulting molar “flow” between intervals is represented by f_i in the figure. Particles can also aggregate, stick together, and form larger particles, as illustrated by $fa_{i,j}$ in the figure. For each interval, there are two components of flow due to aggregation: flow into the interval (fa_i^{in}) and flow out of the interval (fa_i^{out}). Particle attrition can be represented similarly, but it is not addressed in this work. Finally, the amount of particles in a size interval can change if external flows q_i add or remove particles. A general form of the mole balance over a size interval i is then

$$\frac{dM_i}{dt} = f_{i-1} + r_i - f_i + fa_i^{in} - fa_i^{out} + \sum_{\gamma} q_{i,\gamma}, \quad (7)$$

where M_i is the number of moles of silicon particles in an interval.

To use Equation (7) to simulate changes in the particle size distribution, the flow terms ($f_i, r_i, fa_i, \sum_{\gamma} q_{i,\gamma}$) must be defined. External flows q_i are defined by system properties. If the fluidized bed reactor operates continuously, seed particles are added and large particles are removed as product, and these flows affect the size distribution.

The r_i term represents the amount of produced silicon that is distributed to the i^{th} size

interval. So, the total solids production rate defined in Equation (4) is given by the equation

$$R = \sum_i r_i.$$

The rate of moles added to a size interval is in general a function dependent on parameters such as then number of moles in an average particle in the interval (m_i), the number density of particles of a certain size ($N_i/\sum_i N_i$), temperature (T), et cetera, so that

$$r_i = R(m_i, \frac{N_i}{\sum_i N_i}, T, \dots). \quad (8)$$

To simplify model development, it is assumed that the total reaction, R , is distributed among the size intervals according to the fraction of total surface area of silicon particles inside the interval. If A_i represents the total surface area of particles inside a size interval, then the product of reaction that is distributed to that interval is given by

$$r_i = R \cdot \frac{A_i}{\sum_i A_i}. \quad (9)$$

In this work, we assume that the particles are spherical. This corresponds well to experimental sphericity measurements.

The terms, fa_i^{in} and fa_i^{out} , represent the molar flows into and out of size intervals that result from particle aggregation. We assume that particle aggregation depends on binary interactions. We furthermore assume that the molar flow of aggregated particles from the i^{th} and j^{th} size intervals, $fa_{i,j}$, is proportional to the product of concentrations of particles in intervals i and j . This gives

$$fa_{i,j} = k_{i,j}C_iC_j.$$

The concentration C_i is defined to be the moles of silicon in interval i divided by the volume of the reaction zone. The value of $k_{i,j}$ is estimated by comparing model predictions with experimental data.

It is important to distinguish between flow due to aggregation leaving an interval and flow due to aggregation entering an interval. If, particles of size m_i and m_j combine to form a particle of size m_k , then the number of particles leaving interval i is a fraction of the total aggregation flow, $fa_{i,j}$. That fraction is defined by the number of moles in the aggregating particle relative to the

number of moles in the created particle. The total flow out of interval i due to aggregation is the sum of all the interactions with other particles so that

$$fa_i^{out} = \sum_j \left(fa_{i,j} \cdot \frac{m_i}{m_i + m_j} \right). \quad (10)$$

The flow into an interval i depends on the number of moles in particles created by aggregation. The size intervals to which particles created through aggregation belong are determined by comparing the number of moles in particles with the characteristic number of moles of each size interval. Each size interval has a lower bound on moles, m_i^{LB} . If a created particle has more moles than m_i^{LB} and fewer than m_{i+1}^{LB} , then the particle belongs in interval i . The total aggregation flow into an interval can be represented by the expression

$$fa_i^{in} = \sum_j \sum_k fa_{j,k}, \text{ for } m_i^{LB} \leq (m_j + m_k) < m_{i+1}^{LB}. \quad (11)$$

To close the balance equations (7) and develop an expressions for f_i , we use the particle number balance over each size interval. The combination of mass and number balances in this modeling approach is similar to the two-moment method used by Adams & Seinfeld (2002) to discretize and solve the population balance equation. Here the method we develop is computationally simpler since we can eliminate the number balance and develop an analytical expression for f_i . The number of particles in an interval (N_i) can be obtained using

$$N_i = \frac{M_i}{m_i},$$

where again, m_i is the number of moles in an average-sized particle in the interval. An important assumption here is that the number of particles, N_i is a continuous variable. This implies that a relationship between the time derivatives of number and moles of particles can be written

$$\frac{dN_i}{dt} = \frac{1}{m_i} \cdot \frac{dM_i}{dt}. \quad (12)$$

Just as a silicon mole balance over each size interval exists, a particle number balance over each size interval also exists.

$$\frac{dN_i}{dt} = \frac{f_{i-1}}{m_i} - \frac{f_i}{m_{i+1}} + \frac{fa_i^{in}}{m_i} - \frac{fa_i^{out}}{m_i} \quad (13)$$

Here the number of particles flowing in a stream is equal to the molar flow divided by the number of moles in an average-sized particle of the flow. Neglecting external flows and substituting Equations (7) and (13) into Equation (12) gives

$$f_i = r_i \cdot \frac{m_{i+1}}{m_{i+1} - m_i}. \quad (14)$$

To simulate silane decomposition in a fluidized bed reactor with the model, it is necessary to solve a system of ordinary differential equations with defining algebraic expressions. The differential equations (5) and (6) are used to predict changes in the gaseous species. Equation (7) with terms defined by algebraic equations (9), (10), (11), and (14) are used to predict changes in the solid particles. The system of equations is solved with MATLAB's solver, ode15s.

There are adjustable parameters that can improve model predictions through comparison of predictions with experimental data. The amount of homogeneous product (silicon powder) that is scavenged by silicon particles, $k_{sc}C_p$, ranges from zero to the total mass of powder produced. The aggregation proportionality constant, $k_{i,j}$, can be size-dependent and ranges from 0 to 10^{-8} . A convenient way to define $k_{i,j}$, which is also based on empirical evidence, is to assume that small particles aggregate and large ones do not. Consequently, only two parameters, k and I_C , are required. The proportionality constant k indicates the extent to which particles smaller than a critical size, I_C , aggregate. So $k_{i,j}$ is defined as

$$k_{i,j} = \begin{cases} k \forall i, j \leq I_C \\ 0 \forall i, j > I_C. \end{cases} \quad (15)$$

A comparison of model predictions with experimental data for an optimized choice of parameters is presented in Section 5.

4 Relationship to Population Balance Equation

The population balance equation describes particle behavior along the internal and external coordinate axes. The population balance is, in a general form, (Randolph & Larson 1988)

$$\partial n / \partial t + \nabla \cdot \mathbf{v}n - B + D = 0. \quad (16)$$

Here, n represents the particle distribution function. The rate of change of particles along internal and external coordinate axes is represented by $\nabla \cdot \mathbf{v}n$. The birth or death of particles due to particle agglomeration or attrition is represented by the B and D terms respectively.

We now show that the discrete model (7) for growth of silicon particles approaches the continuous population balance equation (16) when the number of size intervals increases. The following derivation based on ones completed by Randolph & Larson (1988) and Kreuzer (1981) illustrates this concept. If the expression (14) for molar flow between size intervals, f_i , is substituted into the size interval mass balance, (7), it is possible to re-write the balance:

$$\frac{dM_i}{dt} = f_{i-1} - \hat{f}_i + f a_i^{IN} - f a_i^{OUT} + \sum_{\gamma} q_{i,\gamma}. \quad (17)$$

If μ represents the continuous mass density distribution over a region Ω of the particle phase space, then the total mass of particles is

$$M_i = \int_{\Omega} \mu d\Omega.$$

The aggregation ‘‘flow’’ terms are source and sink terms, the difference of which may be expressed as

$$f a_i^{IN} - f a_i^{OUT} = \int_{\Omega} (B - D) d\Omega.$$

The flow along the internal coordinate axis, f_i , and the external flow from the surroundings, $\sum_{\gamma} q_{i,\gamma}$ can be written

$$f_{i-1} - \hat{f}_i + \sum_{\gamma} q_{i,\gamma} = \int_{\Omega} \mathbf{v} d\Omega$$

Using these expressions, the interval mass balance can be re-written.

$$\frac{dM_i}{dt} = \frac{d}{dt} \int_{\Omega} \mu d\Omega = \int_{\Omega} \frac{\partial}{\partial t} \mu d\Omega = \int_{\Omega} (B - D) d\Omega + \int_{\Omega} \mathbf{v} d\Omega$$

Since Ω , the region of particle phase space, is arbitrary, the integrand vanishes, and applying the divergence theorem to the flow term gives

$$\frac{\partial \mu}{\partial t} - \nabla \cdot \mathbf{v} = B - D, \quad (18)$$

which is a special case of the population balance equation (16) applicable to our system. We can therefore view Equation (7) and the adjoining constraints as a physically based discretization

scheme for (16).

5 Model Validation

In this section, the model is validated against actual experimental results. Experiments were conducted in a pilot scale fluidized bed reactor at Solar Grade Silicon’s production site in Moses Lake, Washington. A bed of silicon granules were charged, fluidized, and heated to reaction temperature. Then, silane was introduced to the reactor and thermally decomposed, and silicon deposited onto the granules. Usually once per hour, a mass of silicon granules equivalent to the mass of silicon deposited during the hour was removed from the bed. More frequent measurements were not feasible, because an online particle size analyzer, such as the one described by Cooper & Clough (1985), was not developed for the experimental system. The mass and size distribution of each removal was recorded. To investigate changes in the average particle size in certain runs, small particles (seed) were introduced periodically, and the mass removed increased accordingly.

The model estimates periodic change in particle size and mass using experimental reaction conditions. Predicted and actual values of total mass and number of particles that were present in the reactor when a sample was removed at the end of each period during an experiment are shown in Figure 4. When the model does not account for powder loss, the Lai kinetic expressions predict a total mass that is higher than the actual mass. This is expected since experiments indicate that a fraction of the produced silicon is entrained and leaves the reactor with the gas during production. Assigning a positive value to k_{sc} ($0 < k_{sc}C_p < M_p$) enables the model to predict mass much more accurately as shown in Figure 4. The predicted number of particles are estimates at the end of each period based on mass and population balances. The modeled number is actually a continuous parameter. Since the model predicts a number that is too high, it is necessary to account for particle aggregation. Using Equation (15) to define $k_{i,j}$, where $0 < k < 10^{-8}$ and $I_C = 3$, allows the model to predict the number of particles more accurately, as shown in Figure 4. With appropriate values of k_{sc} and $k_{i,j}$, the size distribution is predicted accurately and within the range of uncertainty of the measurement. Figure 5 shows the size distribution of silicon particles obtained near the beginning, middle, and end of an experimental run. Model parameters were the same for all conditions. Many other experimental runs were conducted, and the model exhibited similar behavior. These results show that the efficient discrete interval model provides a practical way to predict the behavior of this process.

6 Sensitivity Analysis Using Feedback Control

A key control parameter in any particulate growth process is size control. Size grows through deposition and agglomeration, which are included in model. Size is reduced through attrition, which is not yet included in the model, and addition of small seed particles. Since small changes in process conditions can upset the fine balance between growth and reduction, it is important to understand long-term effects of process conditions on this performance. As a first approximation, attrition is neglected and size reduction is controlled only through seed addition.

To this end, steady-state simulations incorporating feedback control theory were performed to simulate the mass distribution of silicon particles in the reactor. This was achieved by solving mass balance equations for each discrete size interval. The mass balance for each size interval can be written as

$$\frac{dM_i}{dt} = g_i + \sum_{\gamma} q_{i,\gamma}.$$

Here, $g_i = f_{i-1} + r_i - f_i + fa_i^{IN} - fa_i^{OUT}$ is a function of mass flow between size intervals, and q_i represents external flow rates (seed and product) as shown in Figure 1. The external flow rates control the mass and size distribution of silicon in the reactor. Applying a proportional feedback (K) to keep mass of silicon in the reactor constant at a given set point, M^* , allows definition of the external flow rates.

$$\sum_{i=n_L}^{n_H} q_i = - \sum_{i=n_L}^{n_H} g_i - K \left(\sum_{i=n_L}^{n_H} M_i - M^* \right). \quad (19)$$

The range of size intervals is $1 \leq n_L \leq n_H \leq N$, where N is the largest size interval. If the summations of Equation (19) are performed over all the size intervals, we have $n_L = 1$ and $n_H = N$, and it is possible to define the product flow rate required to maintain a constant total mass of particles.

$$product = - \sum_{i=1}^N g_i - K \left(\sum_{i=1}^N M_i - M^* \right) \quad (20)$$

If the summations of Equation (19) are performed over the seed size intervals, where I_s is the largest seed size interval, then the seeding flow rate required to control the mass of seed particles in the system is

$$seed = - \sum_{i=1}^{I_s} g_i - K \left(\sum_{i=1}^{I_s} M_i - M_s^* \right). \quad (21)$$

Equations (20) and (21) were used to define external flow terms in the model, and we checked

performance sensitivity to various conditions. The steady state mass and flow rates achieved for one scenario are shown in Figure 6. Many of these simulations were performed to produce Figure 7, which illustrates that the average size of the product removed depends on the ratio of the mass of seed particles to the total mass of particles in the reactor. The size simulations were performed for $I_s = 3$. The seed flow rate (21) had a fractional distribution of mass in the first three size intervals of 0.3, 0.3, and 0.4, respectively.

Figure 8 shows that the product size distribution depends on the distribution of the seed added to the reactor as well as the the seed to total mass ratio. Each column represents the product distribution into size intervals 6, 7, and 8 obtained for a given seed flow distribution and a given seed to total mass ratio in the reactor. Large product (size intervals 7 and 8) is obtained when the seed to total mass ratio is low (0.17 or 0.20), as demonstrated in Figure 7. Additionally, the relative amounts of different sizes change with different seed flow distributions.

7 Conclusions

Particle mass and number balances over discrete size intervals were performed to develop a tractable population balance model for size distribution of particulate processes. The model simulates silicon production during thermal decomposition of silane in a fluidized bed reactor. Simulations were compared with experimental data and enabled determination of appropriate values of adjustable parameters that accurately predict powder scavenging as well as particle aggregation. Consequently, the model allows interpretation of growth and losses in a pilot scale unit. The novel sensitivity analysis based on steady-state simulations with feedback control indicate how the product size distribution is influenced by the ratio of seed to total mass and the distribution of seed entering the system. This model will enable development of control strategies and study of dynamic stability of particles' behavior in fluidization processes.

Acknowledgments

This work is supported in part by the National Science Foundation Graduate Research Fellowship Program and Solar Grade Silicon LLC.

List of Symbols

A_i	surface area of average particle of size interval i , m^2
C_h	hydrogen concentration, mol/m^3
C_i	concentration of silicon of size interval i , mol/m^3
C_s	silane concentration, mol/m^3
F	external gas flow, m^3/s
f	particle flow between size intervals, mol/s
fa	particle flow due to aggregation, mol/s
I_C	critical size interval above which particles do not aggregate
$k_{i,j}$	aggregation proportionality constant, $\text{m}^6/(\text{mol}\cdot\text{s})$
k_{sc}	scavenging proportionality constant, m^3/s
M_i	total moles of silicon in size interval i , mol
m_i	number of moles in average particle of size interval i , mol
N_i	total number of silicon particles in size interval i
q	external particle flow, mol/s
r_i	silicon production in size interval i , mol/s
R	silicon production rate, mol/s
T	reaction temperature, K
V_g	reactor gas volume, m^3

References

- Adams, P. J. & Seinfeld, J. H. (2002), ‘Predicting global aerosol size distributions in general circulation models’, *Journal of Geophysical Research* **107**(D19).
- Caussat, B., Hemati, M. & Couderc, J. P. (1995a), ‘Silicon deposition from silane or disilane in a fluidized bed-part i: Experimental study’, *Chemical Engineering Science* **50**(22), 3615–3624.
- Caussat, B., Hemati, M. & Couderc, J. P. (1995b), ‘Silicon deposition from silane or disilane in a fluidized bed-part ii: Theoretical analysis and modeling’, *Chemical Engineering Science* **50**(22), 3625–3635.
- Cooper, D. J. & Clough, D. E. (1985), ‘Experimental tracking of particle-size distribution in a fluidized bed’, *Powder Technology* **44**, 169–177.
- Dueñas Diez, M., Ausland, G., Fjeld, M. & Lie, B. (2002), ‘Simulation of a hydrometallurgical leaching reactor modeled as a dae system’, *Modeling, Identification and Control* **23**(2), 93–115.
- Furusawa, T., Kojima, T. & Hiroha, H. (1988), ‘Chemical vapor deposition and homogeneous nucleation in monosilane pyrolysis within interparticle spaces -application of fines formation analysis to fluidized bed cvd-’, *Chemical Engineering Science* **43**(8), 2037–2042.
- Henson, M. A., Müller, D. & Reuss, M. (2002), ‘Cell population modelling of yeast glycolytic oscillations’, *Biochemical Journal* **368**, 433–446.
- Hogness, T. R., Wilson, T. L. & Johnson, W. C. (1936), ‘The thermal decomposition of silane’, *Journal of the American Chemical Society* **58**, 108–112.

- Hounslow, M. J. (1990), ‘A discretized population balance for continuous systems at steady state’, *AIChE Journal* **36**(1), 106–116.
- Hsu, G., Rohatgi, N. & Houseman, J. (1987), ‘Silicon particle growth in a fluidized-bed reactor’, *AIChE Journal* **33**(5), 784–791.
- Immanuel, C. D. & Doyle III, F. J. (2003), ‘Computationally efficient solution of population balance models incorporating nucleation, growth and coagulation: application to emulsion polymerization’, *Chemical Engineering Science* **58**, 3681–3698.
- Iya, S. K., Flagella, R. N. & DiPaolo, F. S. (1982), ‘Heterogeneous decomposition of silane in a fixed bed reactor’, *Journal of the Electrochemical Society* **129**(7), 1531–1535.
- Kreuzer, H. J. (1981), *Nonequilibrium Thermodynamics and its Statistical Foundations*, Clarendon Press, Oxford.
- Lai, S., Dudokovic, M. P. & Ramachandran, P. A. (1986), ‘Chemical vapor deposition and homogeneous nucleation in fluidized bed reactors: Silicon from silane’, *Chemical Engineering Science* **41**(4), 633–641.
- Randolph, A. D. & Larson, M. A. (1988), *Theory of Particulate Processes*, 2 edn, Academic Press, San Diego.
- Tejero-Ezpeleta, M. P., Buchholz, S. & Mleczko, L. (2004), ‘Optimization of reaction conditions in a fluidized-bed for silane pyrolysis’, *Canadian Journal of Chemical Engineering* **82**, 520–529.
- Weimer, A. W. & Clough, D. E. (1980), ‘Dynamics of particle size/conversion distributions in fluidized beds: Application to char gasification’, *Powder Technology* **26**, 11–16.
- Woditsch, P. & Koch, W. (2002), ‘Solar grade silicon feedstock supply for pv industry’, *Solar Energy Materials & Solar Cells* **72**, 11–26.
- Zambov, L. (1992), ‘Kinetics of homogeneous decomposition of silane’, *Journal of Crystal Growth* **125**, 164–174.

List of Figures

Figure 1. Fluidized bed reactor

Figure 2. Particle phase space

Figure 3. Molar flow through discrete size intervals

Figure 4. Mass and number of silicon particles achieved during reaction

Figure 5. Particle size distribution achieved during reaction

Figure 6. Silicon mass and flow rates for long-term operation

Figure 7. Average product size as a function of M_s/M

Figure 8. Product distribution as a function of seed distribution

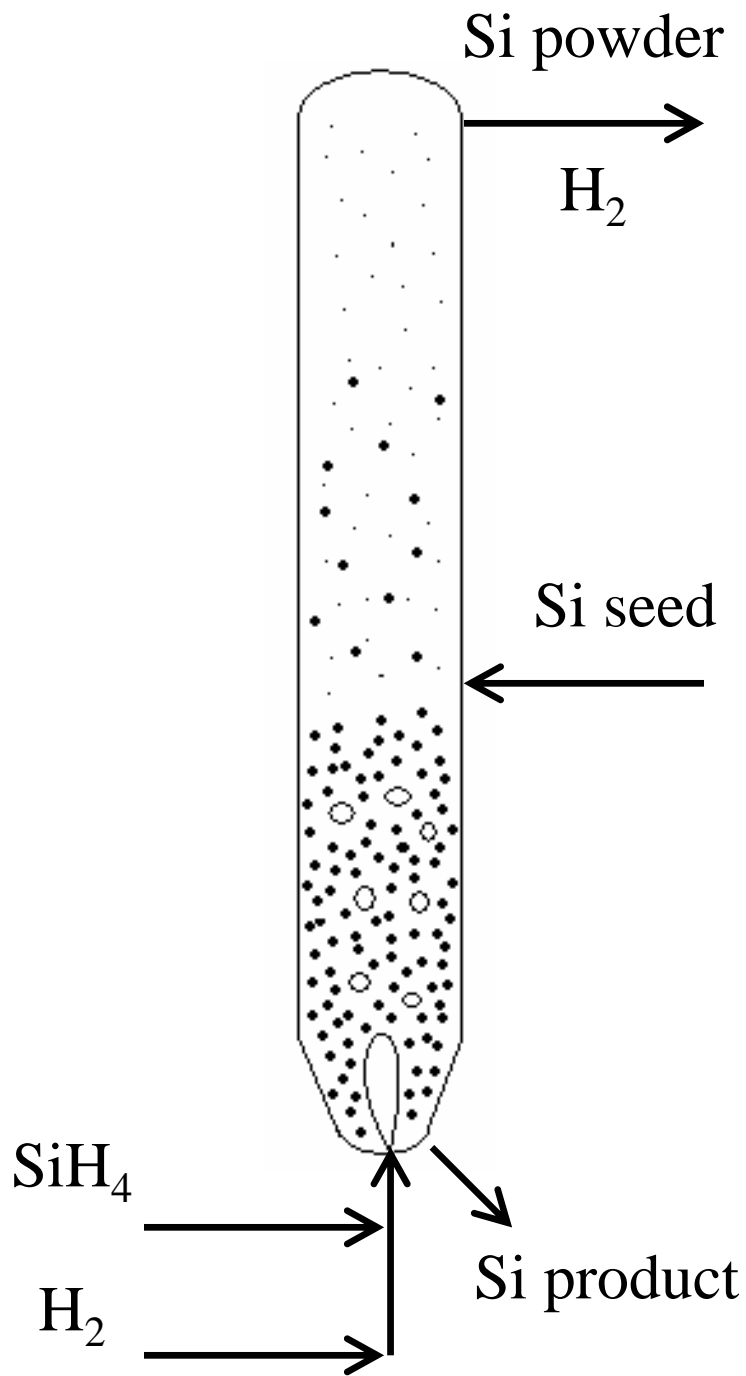


Figure 1: Fluidized bed reactor

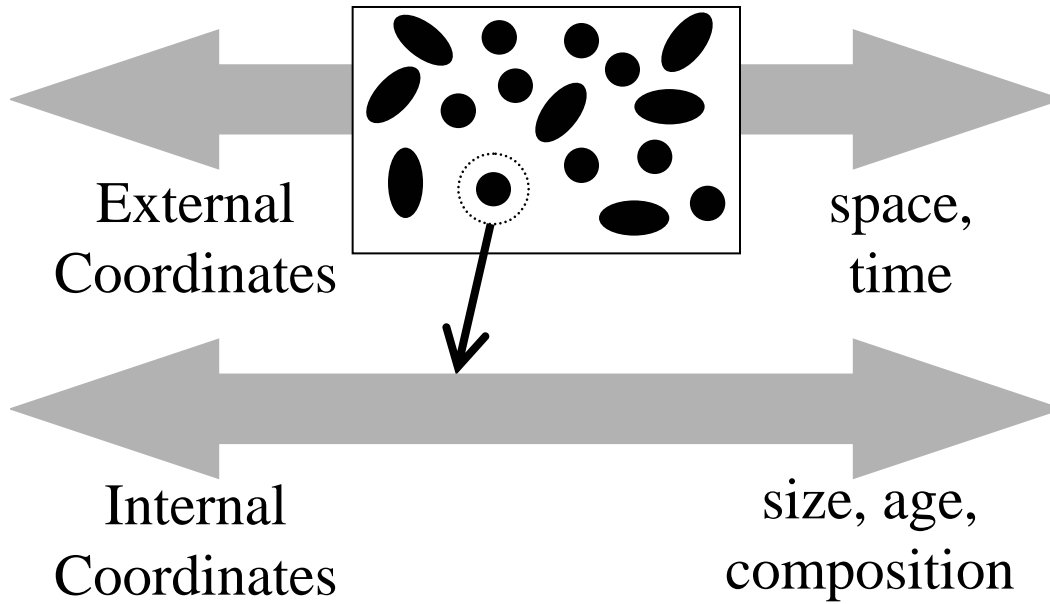


Figure 2: Particle Phase Space

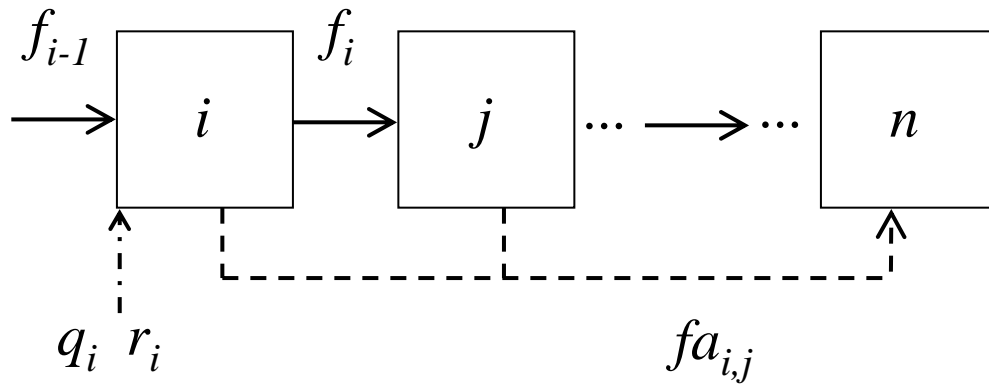


Figure 3: Molar flow through discrete size intervals

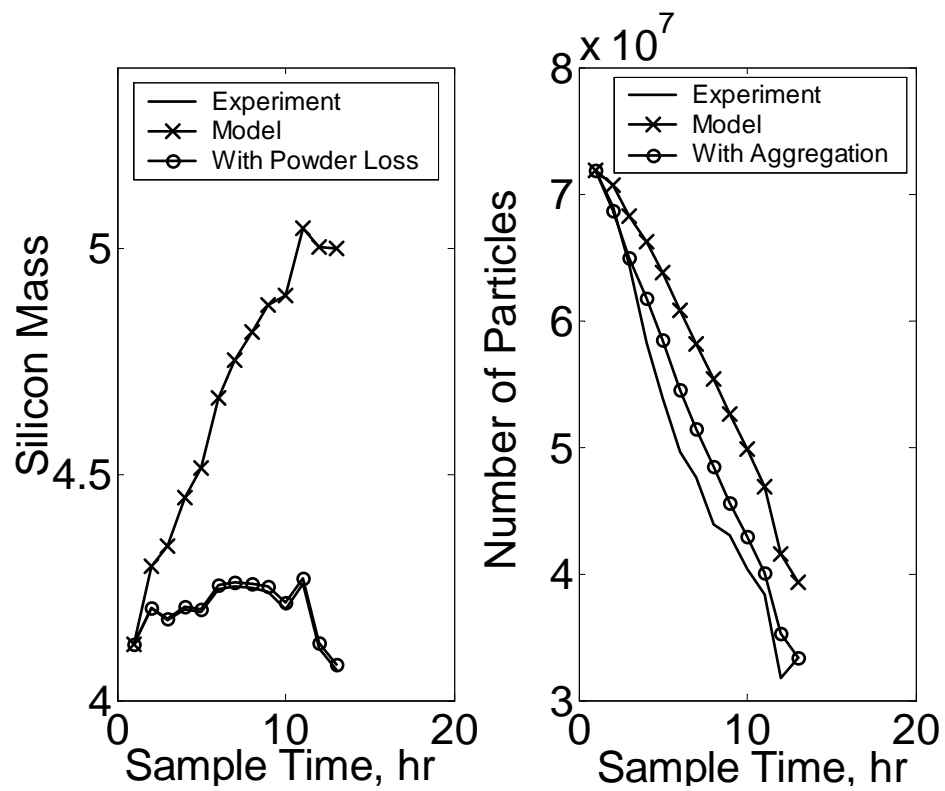


Figure 4: Mass and number of silicon particles achieved during reaction

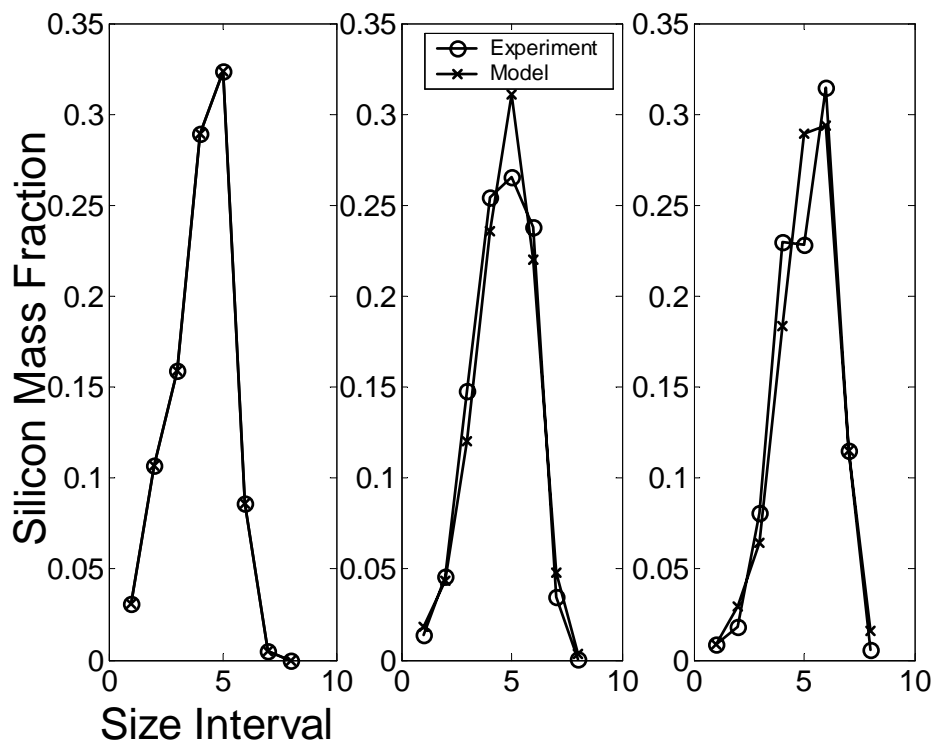


Figure 5: Particle size distribution achieved during reaction

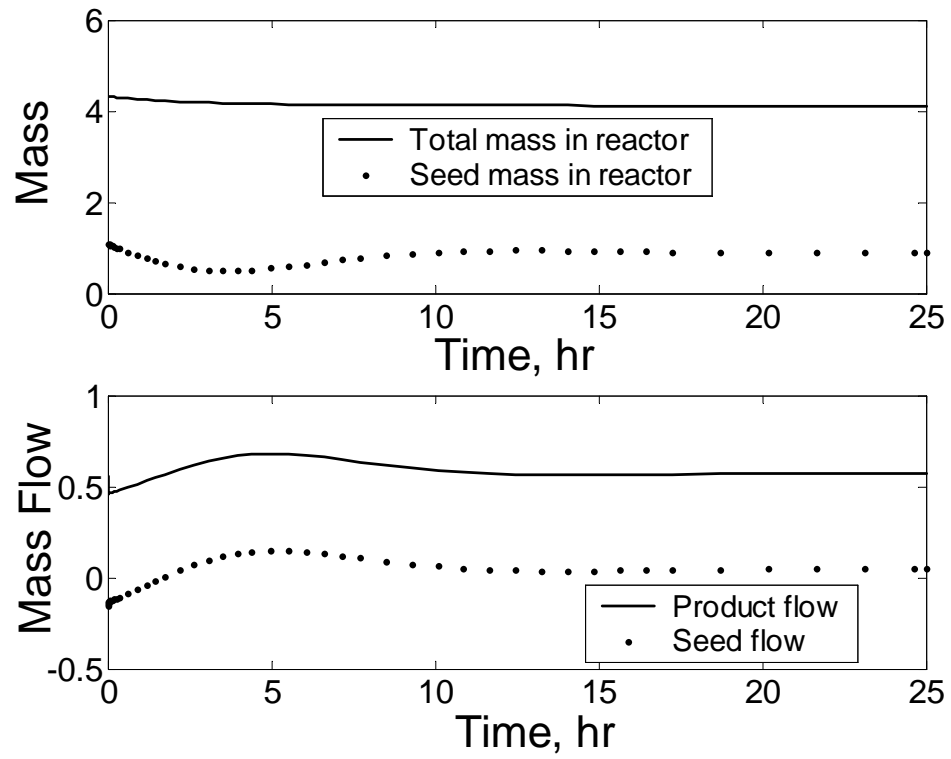


Figure 6: Silicon mass and flow rates for long-term operation

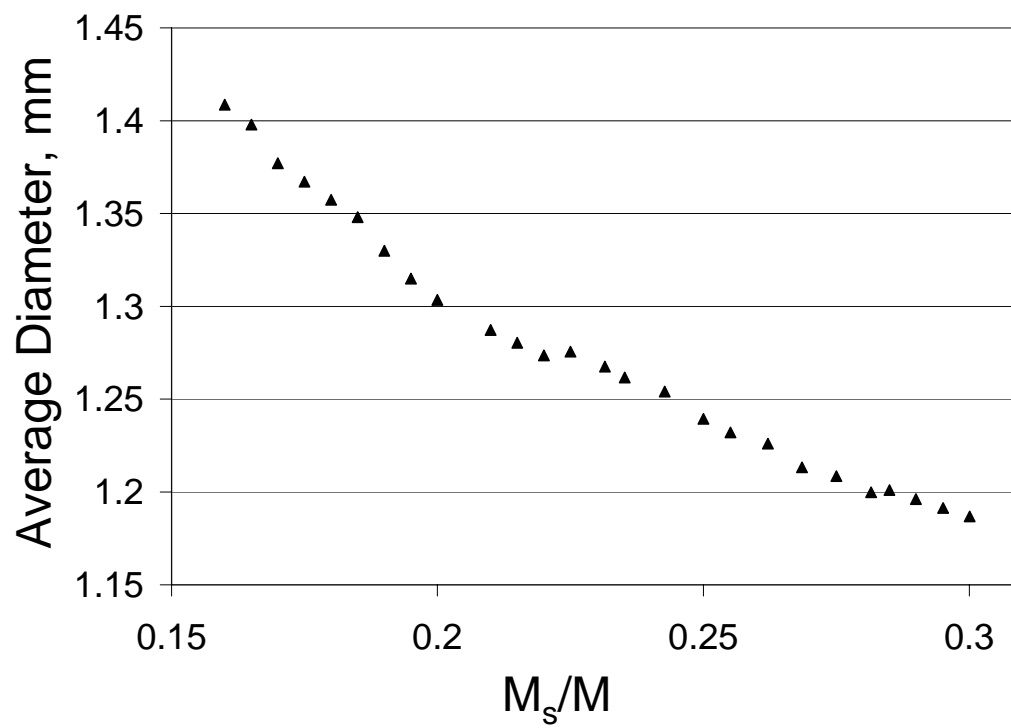


Figure 7: Average product size as a function of M_s/M

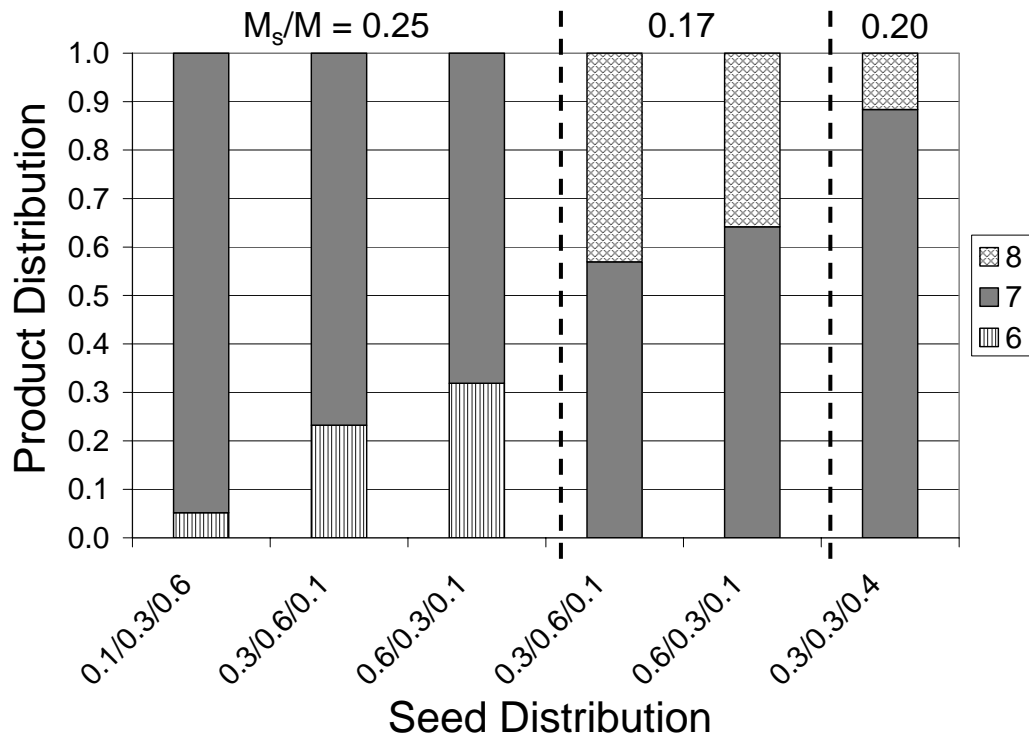


Figure 8: Product distribution as a function of seed distribution